# Self-Assembly and Chemical Reactivity of Alkenes on Platinum Nanoparticles

Peiguang Hu,[†] Paul N. Duchesne,[‡] Yang Song,[†] Peng Zhang,[‡] and Shaowei Chen*,[†]

[†]Department of Chemistry and Biochemistry, University of California, 1156 High Street, Santa Cruz, California 95064, United States
[‡]Department of Chemistry, Dalhousie University, 6274 Coburg Road, Halifax, Nova Scotia B3H 4R2, Canada

ABSTRACT: Stable platinum nanoparticles were synthesized by the self-assembly of alkene derivatives onto the platinum surface, possibly forming platinum—vinylidene (Pt=C=CH−) or −acetylide (Pt−C≡) interfacial bonds as a result of dehydrogenation and trans-formation of the olefin moieties catalyzed by platinum. Transmission electron microscopic measurements showed that the nanoparticles were well-dispersed without apparent agglomeration, indicating effective passivation of the nanoparticles by the ligands, and the average core was estimated to be 1.34 ± 0.39 nm. FTIR measurements showed the emergence of a new vibrational band at 2023 cm^{-1}, which was ascribed to the formation of Pt−H and C≡C from the dehydrogenation of alkene ligands on platinum surfaces. Consistent behaviors were observed in photoluminescence measurements, where the emission profiles were similar to those of alkyne-functionalized Pt nanoparticles that arose from intraparticle charge delocalization between the particle-bound acetylene moieties. Selective reactivity with imine derivatives further confirmed the formation of Pt=C=CH− or Pt−C≡ interfacial linkages, as manifested in NMR and electrochemical measurements. Further structural insights were obtained by X-ray absorption near-edge spectroscopy and extended X-ray absorption fine structure analysis, where the coordinate numbers and bond lengths of the Pt−Pt and Pt−C linkages suggested that the metal−ligand interfacial bonds were in the intermediate between those of Pt−C≡ and Pt−Csp^2.
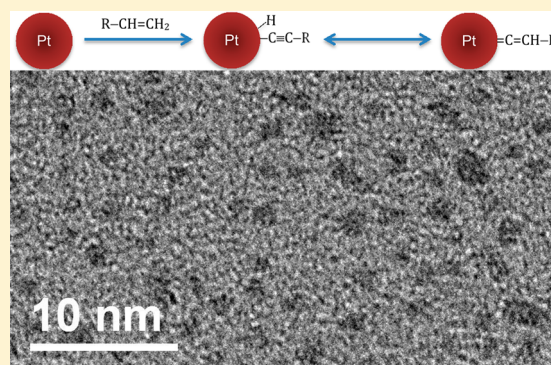
■ INTRODUCTION

Organically capped transition-metal nanoparticles represent a unique class of functional nanomaterials whose material properties have been found to be readily manipulated by the chemical natures of both the metal cores and organic ligands. More recently, metal−ligand interfacial bonding interactions have also been recognized as a powerful and valuable tool in the regulation of the chemical and physical properties of metal nanoparticles, as highlighted by a series of studies in which nanoparticles are functionalized by (conjugated) metal−carbon (or nitrogen) covalent bonds, in contrast with those passivated by mercapto derivatives.[1−4] Several experimental strategies have been developed, for instance, by taking advantage of the self-assembly of diazo derivatives on freshly prepared metal surfaces forming metal−carbene π bonds (M=C), the formation of metal−acetylide (M−C≡) or metal−vinylidene (M=C=CH−) bonds with acetylene derivatives, as well as the formation of metal−nitrene (M=N) π bonds with nitrene derivatives produced by the thermolytic reduction of azides.[1−4] These interfacial bonds are presumed to involve p$_\pi$−d$_\pi$ bonding interactions between the unsaturated ligands and the metal centers,[5] akin to those observed in conventional organometallic complexes.[6,7] In these nanoparticles with conjugated bonds at the metal−ligand interface, extensive intraparticle charge delocalization occurs between particle-bound functional moi-

eties, leading to the emergence of electronic and optical properties that are analogous to those of their dimeric forms. Such unprecedented material properties have been exploited for the sensitive and selective detection of various compounds and ions through deliberate engineering of the nanoparticle surface.[1−4]

With these earlier successes, one immediate question arises: is it possible to functionalize nanoparticles with alkene derivatives? Note that alkene molecules are known to adsorb on transition-metal surfaces, undergoing interfacial structural transformation (isomerization) through dehydrogenation.[5,8] For example, the interaction of ethylene (CH$_2$=CH$_2$) with Pt has been extensively studied as a model system in the investigation of the alkene hydrogenation−dehydrogenation process.[8−10] At low temperatures (< 50 K), ethylene adsorbs onto platinum with the C=C bond parallel to the Pt surface, maintaining largely sp^2 character. However, at higher temperatures, several new and more stable species are generated by structural transformations.[11] For instance, at temperatures above 90 K, rehybridization of the π bond may be induced by electron transfer from Pt into the π* orbital, followed by the

formation of a di-σ bound species on the Pt surface.[10] At higher temperatures, new surface species such as vinyl, vinylidene (~140 K), and ethylidyne (~300 K) may be generated as a result of the dehydrogenation reactions.[10,12] Note that these aforementioned species can coexist on the platinum surface; however, the coverage of each varies with temperature.

Propylene ($CH_3CH=CH_2$) is another small alkene molecule that has attracted extensive interest. For instance, in the study of the interfacial interactions of propylene with platinum using reflection−absorption infrared spectroscopic (RAIRS) techniques, it has been proposed that at least four species might be derived from adsorbed propylene depending on surface coverage and temperature.[13] At temperatures below 230 K, undissociated propylene molecules adsorb on the platinum surface like ethylene, yet at temperatures up to 275 K, it is shown that propylidyne ($CH_3CH_2C\equiv$), an alkylidyne moiety, is formed resulting from the dehydrogenation and rearrangement of the di-σ species, and the details of such conversion are believed to involve a stable and identifiable intermediate (2-propyl, $CH_3CH(Pt)CH_3$) or propylidene ($Pt=CHCH_2CH_3$).[13] At room temperature, there is evidence showing that propylene exhibits a structure similar to that of ethylene.[14]

For longer alkenes, it has also been proposed that they may decompose through the corresponding alkylidyne intermediates as they adsorb onto the surface of transition-metal surfaces.[14] This is the primary motivation of the present study. Herein we describe the synthesis and characterization of alkene-functionalized platinum nanoparticles. "Bare" Pt colloids were synthesized by thermolytic reduction of Pt(II) in 1,2-propanediol at controlled temperatures. Alkene derivatives were then added to the solution for nanoparticle surface functionalization. The resulting nanoparticles were found to be readily soluble in apolar organic solvents and exhibited apparent photoluminescence emission, suggesting the formation of conjugated metal−ligand interfacial bonds most probably through dehydrogenation reactions of the alkene ligands, a behavior analogous to those of nanoparticles functionalized by acetylene derivatives.[3] The structures of the resulting nanoparticle were characterized by a range of experimental tools including transmission electron microscopy, infrared, photoluminescence, NMR spectroscopy, and electrochemistry. Further structural insights were obtained in X-ray absorption measurements, wherein X-ray absorption near edge spectroscopy (XANES) and extended X-ray absorption fine structure (EXAFS) analyses were carried out to probe the interfacial bonding interactions by using platinum nanoparticles stabilized by trifluoromethylphenyl fragments (PtTFPB, dia. 2.20 nm),[15] dodecyne-stabilized platinum (PtHC12, dia. 1.34 nm) nanoparticles,[3] and a Pt foil as the controls.

■ EXPERIMENTAL SECTION

Chemicals. Platinum chloride ($PtCl_2$, 99+%, ACROS), 1-octadecene (ODE, 98%, ACROS), 1-dodecyne (HC12, 98%, Sigma-Aldrich), 1,2-propanediol (ACROS), sodium acetate trihydrate ($NaOAc \cdot 3H_2O$, MC&B), and potassium trichloro(ethylene)platinate-(II) hydrate (Zeise's salt, $K[Cl_3Pt(C_2H_4)]$, Sigma-Aldrich) were all used as received. The synthesis and characterization of [[(1-methylethyl)imino]methyl]ferrocene (Fc-imine) have been described previously.[2] All solvents were obtained from typical commercial sources and used without further treatment. Water was supplied by a Barnstead Nanopure water system (18.3 MΩ·cm).

Synthesis of Platinum Nanoparticles. Platinum nanoparticles capped by alkene derivatives were prepared by adopting a procedure

that was used previously.[3] In brief, 0.1 mmol of $PtCl_2$ was dissolved in 3 mL of concentrated hydrochloric acid (12.1 M); then, the prepared solution was condensed to 1 mL, neutralized with sodium carbonate, and centrifuged to remove undissolved salts. The supernatant and 1 mmol of NaOAc were added to 100 mL of 1,2-propanediol. The mixed solution was heated to 165 °C under vigorous stirring and kept for 1 h. After the colloid solution was cooled to room temperature, 0.3 mmol of 1-octadecene (at a three-fold molar excess of $PtCl_2$) dissolved in 50 mL of toluene was added, and the mixed solution was stirred magnetically for 7 days. The toluene phase was then collected, dried with rotary evaporation, and rinsed extensively with a copious amount of acetonitrile to remove excessive ligands. The resulting nanoparticles were denoted as PtODE.

Platinum nanoparticles capped by 1-dodecyne (PtHC12) were prepared in a similar fashion except that 1-dodecyne was used instead for nanoparticle surface functionalization and extraction.[3]

The synthesis of platinum nanoparticles stabilized by trifluoromethylphenyl fragments (PtTFPB, dia. 2.20 nm) has been detailed previously by the coreduction of H_2PtCl_4 and trifluoromethylphenyl diazonium salts.[15] In brief, the diazonium salts were synthesized from *para*-trifluoromethylphenyl aniline (0.5 mmol), sodium nitrite (0.52 mmol), and 35% perchloric acid (0.45 mL) in an ice-water bath. The resulting diazonium salt and H_2PtCl_4 (0.1 mmol) were codissolved in a mixed solvent of H_2O-THF (1:1 V/V) into which a freshly prepared $NaBH_4$ solution (0.2 M, 5 mL) was added slowly under magnetic stirring, leading to the formation of a dark brown solution that signified the production of aryl-stabilized Pt nanoparticles.[16,17]

Reactivity of Platinum Nanoparticles. The reactivity of the PtODE nanoparticles prepared above was tested with Fc-imine.[2] Experimentally, 4 mg of PtODE nanoparticles and 12 mg of Fc-imine were codissolved into 2 mL of dry CH_2Cl_2 under vigorous stirring for 7 days. Upon the completion of the reaction, the solution was dried by rotary evaporation and rinsed with acetonitrile for several times to remove excessive free ligands.

Characterization. The morphology and size of the Pt nanoparticles were characterized by transmission electron microscopy studies (TEM, Philips CM300 at 300 kV). ^{1}H NMR spectroscopic measurements were carried out with a Varian Unity Inova 600 MHz NMR spectrometer. UV−vis spectroscopic studies were performed with an ATI Unicam UV4 spectrometer using a 1 cm quartz cuvette with a resolution of 1 nm. Photoluminescence characteristics were examined with a PTI fluorospectrometer. FTIR measurements were carried out with a PerkinElmer FTIR spectrometer (Spectrum One, spectral resolution 4 cm^{-1}), where the samples were prepared by casting the particle solutions onto a ZnSe disk.

X-ray absorption spectroscopic (XAS) studies were performed using the PNC-CAT bending magnet beamline (Sector 20) of the Advanced Photon Source at Argonne National Laboratory, IL. A Si(111) double-crystal monochromator with Rh-coated focusing mirrors was employed for wavelength selection; the incident beam was further detuned to 80% of maximum flux to reject higher harmonics. Data were acquired in fluorescence mode using a liquid-nitrogen-cooled, 32-element Ge detector, with a Pt foil and gas ionization chambers used for in-line energy calibration. To enhance EXAFS signal intensity, measurements were performed at controlled temperatures. Data processing and EXAFS fitting were performed using WinXAS software,[18] and the amplitude and phase scattering factors used in the fits were obtained from model structures using FEFF8.[19] To fit the k^3-weighted EXAFS spectra, a two-stage process was implemented. In the first stage, the energy shift (ΔE_0) and Debye−Waller coefficient (σ^2) values of all scattering paths were correlated to obtain a reasonable starting value for the coordination number (CN) of the Pt−C path. In the second stage, this CN was fixed while allowing the σ^2 values to vary independently, and a single ΔE_0 value was again used to obtain the final fit. Uncertainty in parameter values was determined by weighting the corresponding off-diagonal matrix elements by the reduced χ^2 value of the fit while also taking into consideration shot noise in the Fourier-transformed EXAFS spectrum (15−25 Å).[20]

Electrochemistry. Voltammetric measurements were carried out with a CHI 440 electrochemical workstation. A polycrystalline gold

disk electrode (sealed in glass tubing) was used as the working electrode. A Ag/AgCl wire and a Pt coil were used as the reference and counter electrodes, respectively. The gold electrode was first polished with alumina slurries of 0.5 μm and then cleaned by sonication in 0.1 M HNO$_3$, H$_2$SO$_4$, and Nanopure water successively. Prior to data collection, the electrolyte solution was deaerated by bubbling ultrahigh-purity N$_2$ for at least 20 min and blanketed with a nitrogen atmosphere during the entire experimental procedure.

■ RESULTS AND DISCUSSION

Figure 1 depicts a representative TEM micrograph of the PtODE nanoparticles. It can be seen that the nanoparticles are
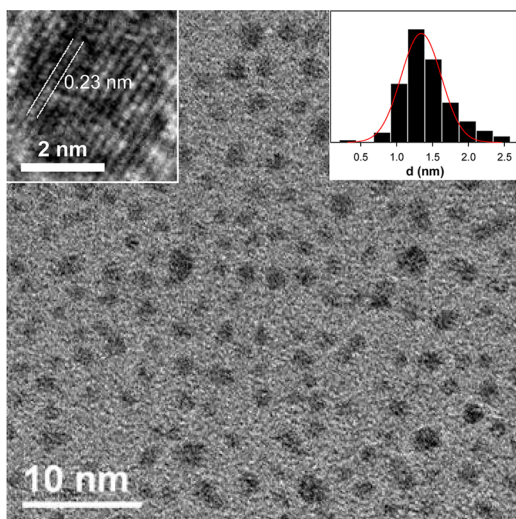

Figure 1. Representative TEM image of platinum colloids prepared by thermolytic reduction of PtCl$_2$ in 1,2-propanediol. Scale bar 10 nm. Upper left inset is a high-resolution TEM image where the lattice fringes of a nanoparticle can be seen at a spacing of 0.23 nm, corresponding to Pt(111) crystal planes. Scale bar 2 nm. Upper right inset shows the nanoparticle core size histogram. Red curve is the Gaussian fit.

well-separated without apparent aggregation, suggesting sufficient protection of the nanoparticles by the capping ligands, and the majority of the nanoparticles are within the narrow range of 1 to 2 nm in diameter, with the average core diameter of 1.34 ± 0.39 nm, as depicted in the right inset. Additionally, from high-resolution imaging in the left inset, one can see that the nanoparticles exhibit clearly defined lattice fringes and the interlayer spacing of 0.23 nm is consistent with the (111) crystal planes of *fcc* platinum (PDF Card 4-802).

The formation of Pt nanoparticles was also manifested in UV−vis absorption measurements, as shown in the inset to Figure 2. The largely featureless exponential decay profile is in good agreement with the Mie scattering of nanosized Pt colloids.[21] Interestingly, the resulting PtODE nanoparticles exhibit apparent photoluminescence. Figure 2 shows the excitation and emission spectra of the PtODE nanoparticles, with a clearly defined excitation peak (λ_{ex}) at 360 nm and an emission peak (λ_{em}) at 452 nm. Note that in a previous study with alkyne-functionalized Pt nanoparticles (such as 1-dodecyne-capped Pt nanoparticles, PtHC12),[3] similar photoluminescence features were observed at λ_{ex} = 352 nm and λ_{ex} = 430 nm, which was accounted for by the formation of Pt−C≡ interfacial bonds such that the particle-bound acetylene moieties behaved analogously to diacetylene derivatives (C≡C−C≡C). In the present study, the fact that the resulting
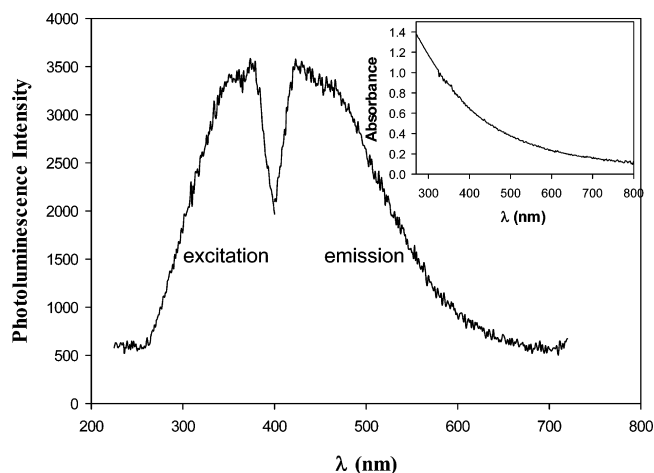

Figure 2. Excitation and emission spectra of PtODE nanoparticles in CH$_2$Cl$_2$. Inset shows the corresponding UV−vis absorption spectrum.

nanoparticles exhibit apparent photoluminescence suggests that a similar interfacial linkage was formed, possibly as a result of dehydrogenation of the alkene ligands on the nanoparticle surface. That is, it is likely that the eventual nanoparticle-bound ligands involved either vinylidene or alkynyl species in which the conjugated interfacial bonds led to intraparticle charge delocalization and hence photoluminescence, as observed previously with alkyne-capped nanoparticles.[5,8,14] Note that the formation of vinylidene species has indeed been confirmed for ethylene molecules absorbed on single-crystal Pt surfaces.[12−14] Such a hypothesis is also supported by a control experiment with Zeise's salt, K[PtCl$_3$(C$_2$H$_4$)], where an olefin is coordinated to the Pt(II) metal center in an η^2 configuration by d$_\pi$−p$_\pi$ interactions.[22,23] The fact that no photoluminescence was observed with Zeise's salt indicates that no such structure was formed at the metal−ligand interface in PtODE nanoparticles.

The structures of the PtODE nanoparticles were further examined by FTIR measurements. Figure 3 depicts the FTIR
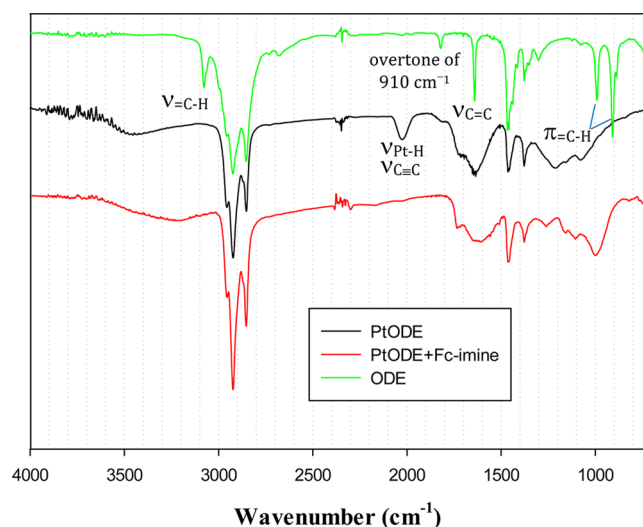

Figure 3. FTIR spectra of PtODE nanoparticles (black curve) and monomeric ODE (green curve). The spectrum of the PtODE nanoparticles after reacting with Fc-imine is also shown as the red curve.

spectra of monomeric ODE ligands and PtODE nanoparticles. For monomeric ODE (green curve), several characteristic bands can be identified at 3077 cm^{-1} for the $=$C$-$H stretch, 1641 cm^{-1} for the C$=$C stretch, and 995 and 910 cm^{-1} for the out-of-plane $=$C$-$H bends (with an overtone of the 910 cm^{-1} absorption at 1817 cm^{-1}).[24] In contrast, the stretching and bending vibrations of the terminal $=$C$-$H groups vanished with the PtODE nanoparticles (black curve; the broad band centered 3500 cm^{-1} most likely arose from residual water), signifying drastic structural transformations of the ODE ligands when bound onto the Pt nanoparticles. Note that in Zeise's salt, the C$=$C stretching vibration is typically found at 1526 cm^{-1}.[25] The absence of such a feature with the PtODE nanoparticles also suggests that it is unlikely that the ODE ligands were bound onto the Pt nanoparticle surface in the η^2 configuration. Concurrently, a new broad peak emerged at ~2023 cm^{-1} that has been previously observed with alkyne-functionalized Pt nanoparticles and ascribed to the combined contributions from nanoparticle-bound C$\equiv$C stretching[1,3,26,27] and Pt$-$H vibrations.[28,29] This suggests that the ODE ligands, at least in part, underwent dehydrogenation reactions on the Pt surface to form acetylide derivatives and, hence, Pt$-$C$\equiv$ bonds, as depicted in Scheme 1. Note that the dehydrogenation reactions of alkenes

Scheme 1
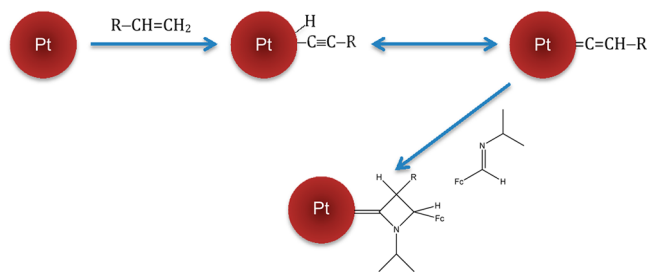
on platinum surfaces are rather complex, involving a range of reaction species.[13,15−17] Therefore, the formation of other dehydrogeneration products at the interface, which are likely spectroscopically silent within the present experimental context, cannot be excluded.

Such a structural model is further confirmed by the selective reactivity of the PtODE nanoparticles with imine derivatives. As previously demonstrated with alkyne-functionalized ruthenium nanoparticles,[2] the metal−acetylide interfacial bonds may be involved in a dynamic equilibrium with metal−vinylidene linkages through a tautomeric rearrangement process, which has been known to react selectively with imine derivatives to form a heterocyclic azetidinylidene complex (Scheme 1).[1,30] We used a ferrocene-imine (Fc-imine) derivative as the illustrating example where the redox-active ferrocenyl moiety might be exploited as a molecular probe. Figure 4 shows the ^{1}H NMR spectra of the PtODE nanoparticles before and after reaction with Fc-imine. It can be seen that for the as-prepared PtODE nanoparticles (black curve), a prominent broad peak appears at ~0.9 ppm, which can be assigned to the terminal methyl (CH$_3$) protons of the ODE ligands, and (part of) the methylene (CH$_2$) protons can be identified by the peak centered at 1.2 ppm. The peak centered at 1.5 ppm can be assigned to protons of residual H$_2$O in the sample, and the three tiny peak around 1.8, 3.5, and 3.7 ppm can be ascribed to protons from residual acetonitrile, methanol, and ethanol, respectively; however, no olefin protons can be seen, which are
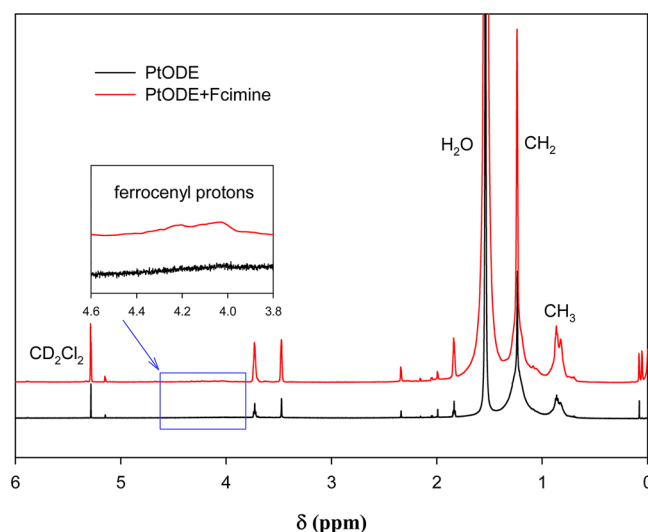

Figure 4. ^{1}H NMR spectra of PtODe nanoparticles before and after reactions with Fc-imine in CD$_2$Cl$_2$. Inset is an enlarged view of the section between 3.8 and 4.6 ppm.

anticipated to appear at about 4.9 and 5.8 ppm.[31] These observations indicate that the nanoparticles were spectroscopically clean and free of any excess ligands, and, importantly, that the olefin moieties are indeed the anchoring groups that bind to the nanoparticle surface. This most probably occurs via their platinum-catalyzed dehydrogenation into acetylene derivatives, where the close proximity to the nanoparticle core surface causes the signals of relevant protons to be broadened into the baseline.[32−35] A very consistent spectral profile was observed for the PtODE nanoparticles after reactions with Fc-imine (red curve), except that an additional broad peak emerged within the range of 3.9 to 4.3 ppm, as illustrated in the Figure inset, which is consistent with the ferrocenyl ring protons; and based on the integrated peak areas of the ferrocenyl and methyl protons, the ferrocene surface concentration was estimated to be 4.3%.[1,30] Again, the absence of any sharp NMR feature indicates that the ferrocenyl moieties were indeed incorporated onto the nanoparticle surface, most likely by the imido transfer reactions (Scheme 1), with no contributions from ferrocenyl monomers.[2] This behavior may be accounted for by the self-assembly of the ODE ligands onto the Pt nanoparticle surface, which then underwent dehydrogenation reactions to form Pt−acetylide interfacial bonds, thus causing the nanoparticles to behave analogously to those functionalized by acetylene derivatives.[2]

The unique reactivity of PtODE nanoparticles with Fc-imine was also manifested in FTIR measurements. From Figure 3, one can see that after the reaction of PtODE nanoparticles with Fc-imine (red curve) the vibration band at 2030 cm^{-1} vanished as a result of imido transfer at the metal−ligand interface where the platinum−acetylide and −hydride bonds disappeared (Scheme 1). The successful incorporation of the ferrocenyl moieties onto the PtODE nanoparticle surface was further evidenced by electrochemical measurements in DMF with 0.10 M tetrabutylammonium perchlorate (TBAP) as the supporting electrolyte. Figure 5 shows the square-wave voltammograms (SWVs) of PtODE nanoparticles (black curve) before and (red curve) after reactions with Fc-imine. In contrast with the featureless voltammetric responses of the as-prepared PtODE nanoparticles, a pair of well-defined voltammetric peaks can be seen with a formal potential of +0.39 V (vs Ag/AgCl) for the
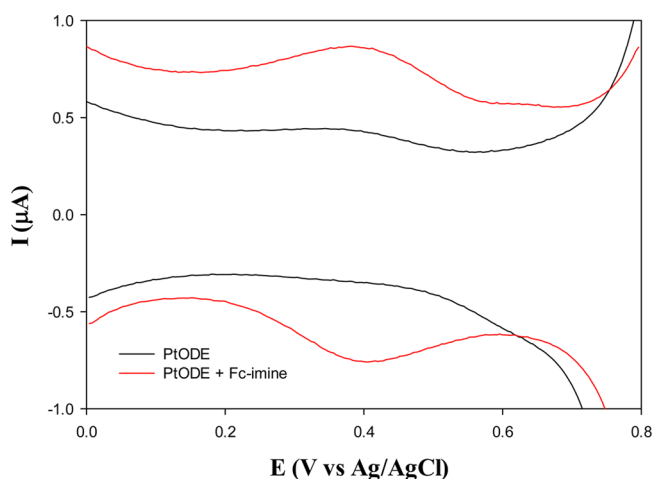
Figure 5. SWVs of PtODE (black curve) before and (red curve) after reactions with Fc-imine in DMF with 0.1 M TBAP. Nanoparticle concentration 2 mg/mL, gold electrode surface area 1.57 mm^2, DC ramp 4 mV/s, and pulse amplitude 25 mV.

PtODE nanoparticles after reaction with Fc-imine. This can be ascribed to the redox reactions of the ferrocenyl moieties incorporated onto the PtODE nanoparticle surface (Fc$^+$ + e$^-$ ↔ Fc). The relatively large peak splitting ($\Delta E_p \approx 20$ mV) may be ascribed to the surrounding of the ferrocenyl moieties by the long aliphatic hydrophobic ligands, as the energetically unfavorable environment would render it difficult for counterions to reach the resulting ferrocenium ions and hence impede the electron-transfer kinetics.[36]

X-ray absorption spectroscopy was then employed to probe the local atomic structure and interfacial Pt-ligand bonding of the PtODE nanoparticles. Figure 6a depicts the X-ray absorption near-edge spectrum (XANES) at the Pt L$_3$ absorption edge of the PtODE nanoparticles, along with those of PtTFPB (dia. 2.20 nm)[15] and PtHC12 (dia. 1.34 nm) nanoparticles,[3] and a Pt foil. There are several aspects that warrant attention here. First, it can be seen that the Pt L$_3$ absorption edges of the three nanoparticles were all apparently shifted to a higher binding energy than that of the Pt foil: PtTFPB (11.566 keV) > PtODE ≈ PtHC12 (11.565 keV) > Pt foil (10.564 keV). Similar behaviors have also been observed in XPS measurements, wherein a blue shift of the binding energy is typically observed of the core and valence electrons for transition-metal nanoparticles relative to those of their bulk counterparts. This is largely accounted for by the interplay between the effects of quantum confinement (nanoparticle size) and reduction of surface coordination.[37] It is interesting to note that whereas the PtODE and PtHC12 nanoparticles are smaller than PtTFPB, the more positively shifted Pt L$_3$ absorption edge of the latter is likely due to the strong electron-withdrawing trifluoromethyl (CF$_3$) moieties.

Second, the intense XANES peak following the absorption edge (the white line) arises from occupied Pt 2p to unoccupied 5d electronic transition, and a more intense white line corresponds to a lower d-electron density.[38,39] From Figure 6a, the white line peak intensity and breadth can be seen to increase in the order of PtHC12 < Pt foil < PtODE < PtTFPB, suggesting a progressive decrease in the Pt d-electron density.[38] Note that extensive intraparticle charge delocalization occurs in PtHC12 nanoparticles between the particle-bound C≡C moieties, with the metal cores as the conducting media.[3]
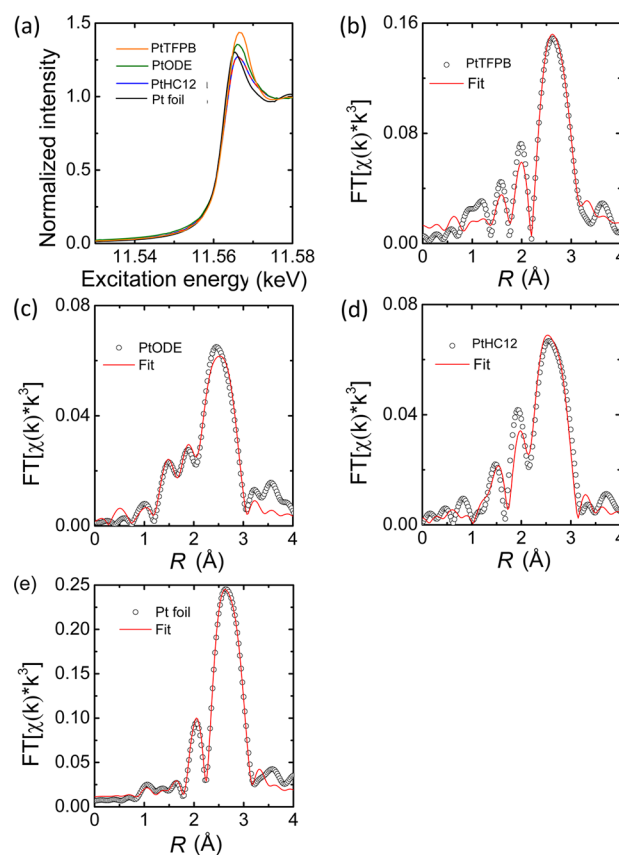

Figure 6. (a) XANES and (b−e) Fourier-transformed EXAFS spectra of PtTFPB, PtODE, and PtHC12 nanoparticles and a Pt foil reference acquired at the Pt L$_3$ absorption edge. Symbols are experimental data and red curves are the corresponding fits.

Spectroscopic studies suggest a marked diminishment of the acetylene bonding order, wherein the conjugated metal−ligand interfacial bonds likely involve partial filling of the empty Pt d orbitals by ligand π electrons, leading to a decrease in the white line intensity as compared with that of bulk Pt. In contrast, the number of unoccupied Pt d states in the PtTFPB nanoparticles was likely enhanced by the strong electron-withdrawing trifluoromethyl moieties, such that the corresponding white line peak intensity was the highest among the series. The fact that the PtODE nanoparticles fell in the intermediate range signifies that the interfacial bonding order was most likely in between that of PtHC12 (Pt=C=CH−/Pt−C≡) and PtTFPB (Pt−Csp$_2$), implying that indeed various dehydrogenation products were formed when the alkene ligands were bound onto the Pt nanoparticle surface in PtODE (Scheme 1).[10,12−14]

In addition to the electronic information gleaned from XANES analysis, significant structural information may also be obtained by examining the extended X-ray absorption fine structure (EXAFS) data. Fitting of the Fourier-transformed EXAFS spectra in panels b−e was then carried out to extract parameters pertinent to the local structure of the samples, with the corresponding parameter values summarized in Table 1. It can be seen that in comparison with bulk Pt (Pt foil) where the Pt−Pt coordination number (CN) is 12, the CN values are much lower for the nanoparticle samples, lying only in the narrow range of 5 to 6. Such low CNs are often observed in nanoparticles due to their relatively large number of low-coordinate surface atoms and are reflective of their nanoscale

Table 1. Structural Parameters Obtained from Fitting of the Pt L$_3$-Edge Fourier-Transformed EXAFS Spectra

bond	PtTFPB		PtODE		PtHC12		Pt foil
	Pt–C	Pt–Pt	Pt–C	Pt–Pt	Pt–C	Pt–Pt	Pt–Pt
CN	0.8	5.2(8)	0.9	6.3(4)	0.8	6.0(1)	12
R (Å)	2.05(5)	2.750(6)	2.01(1)	2.690(4)	1.91(3)	2.72(1)	2.767(2)
σ^2 (Å^2)	0.006(6)	0.0023(7)	0.003(2)	0.0081(4)	0.003(3)	0.007(1)	0.0043(2)
ΔE_0 (eV)	4(1)		-1(1)		2(3)		5.2(5)

dimensions.[39] Consistent behaviors were also observed in the estimation of the Pt–Pt bond length, which was 2.75 Å for PtTFPB, 2.69 Å for PtODE, and 2.72 Å for PtHC12, all slightly smaller than that of bulk Pt (2.77 Å). This may be accounted for by lattice contraction of nanosized particles.[37]

Furthermore, it can be seen from Table 1 that the average Pt–C CN of PtODE nanoparticles is 0.9, which is close to that of the PtTFPB and PtHC12 nanoparticles (0.8). Note that based on a truncated octahedral core structure and the average nanoparticle core diameter the fraction of surface atoms might be estimated to be 87.3% for PtODE and PtHC12 and 57.2% for PtTFPB.[40] This signifies that the number of ligands bound to each surface Pt atom is ~1.03 for PtODE, 0.92 for PtHC12, and 1.53 for PtTFPB nanoparticles. That is, the nanoparticles were all capped densely by the respective organic capping ligands. In fact, TEM measurements (Figure 1) showed good dispersion of the nanoparticles without apparent agglomeration, signifying effective passivation of the nanoparticles by the organic capping ligands.

Further structural insights can be obtained from analysis of the mean Pt–C bond length. As depicted in Table 1, the Pt–C bond length is determined to be 2.05 Å for PtTFPB nanoparticles that feature largely Pt–Csp^2 single bonds[15] and 1.91 Å for PtHC12 nanoparticles that are known to exhibit a Pt=C=CH–/Pt–C≡ interfacial bond.[3] Note that these are in very good agreement with results in a previous study of diplatinum complexes with C8 and C12 sp carbon chains where the Pt–C≡ bond length was estimated to be 1.99 Å and that of Pt–Csp^2 was estimated to be 2.06 Å.[41] For PtODE nanoparticles the Pt–C bond length from EXAFS is 2.01 Å, which is in the intermediate between those of PtTFPB and PtHC12, suggesting that the bonding order is between those of Pt–C≡ and Pt–Csp^2. Again, this is likely due to the formation of various interfacial structures of the ODE ligands on the Pt surfaces (e.g., alkenes, alkylidenes, alkylidynes, etc.), some of which were spectroscopically silent within the present experimental context.[13,14] Finally, one may notice that when ethylene is adsorbed on Pt(111) surfaces forming di-σ interfacial bonds, the Pt–C bond length is estimated to be at least 2.21 Å, markedly larger than those observed here with the three nanoparticles.[42]

CONCLUSIONS

Stable platinum nanoparticles were successfully prepared by the functionalization of alkene derivatives. Spectroscopic measurements suggested that at least part of the alkene ligands underwent dehydrogenation reactions on the platinum nanoparticle surface forming Pt=C=CH–/Pt–C≡ interfacial bonds, a structure that was identified when alkynes were self-assembled onto the nanoparticle surface. Further structural insights were obtained from X-ray absorption measurements, which indicated that the effective metal–ligand interfacial bonds were most likely in the intermediate between those of Pt–C≡ and Pt–Csp^2. Results from this study further enhance

the "tool box" for nanoparticle surface functionalization, where increasingly complicated manipulation of their structures and properties may be achieved.

AUTHOR INFORMATION

Corresponding Author
*E-mail: shaowei@ucsc.edu.

Notes
The authors declare no competing financial interest.

REFERENCES

(1) Chen, W.; Zuckerman, N. B.; Kang, X. W.; Ghosh, D.; Konopelski, J. P.; Chen, S. W. Alkyne-Protected Ruthenium Nanoparticles. *J. Phys. Chem. C* **2010**, *114*, 18146−18152.

(2) Kang, X. W.; Zuckerman, N. B.; Konopelski, J. P.; Chen, S. W. Alkyne-Functionalized Ruthenium Nanoparticles: Ruthenium-Vinylidene Bonds at the Metal-Ligand Interface. *J. Am. Chem. Soc.* **2012**, *134*, 1412−1415.

(3) Liu, K.; Kang, X. W.; Zhou, Z. Y.; Song, Y.; Lee, L. J.; Tian, D.; Chen, S. W. Platinum nanoparticles functionalized with acetylene derivatives: Electronic conductivity and electrocatalytic activity in oxygen reduction. *J. Electroanal. Chem.* **2013**, *688*, 143−150.

(4) Kang, X. W.; Song, Y.; Chen, S. W. Nitrene-functionalized ruthenium nanoparticles. *J. Mater. Chem.* **2012**, *22*, 19250−19257.

(5) Zaera, F. An organometallic guide to the chemistry of hydrocarbon moieties on transition metal surfaces. *Chem. Rev.* **1995**, *95*, 2651−2693.

(6) Koestner, R. J.; Vanhove, M. A.; Somorjai, G. A. Molecular-Structure of Hydrocarbon Monolayers on Metal-Surfaces. *J. Phys. Chem.* **1983**, *87*, 203−213.

(7) Belluco, U.; Bertani, R.; Michelin, R. A.; Mozzon, M. Platinum-alkynyl and -alkyne complexes: old systems with new chemical and physical perspectives. *J. Organomet. Chem.* **2000**, *600*, 37−55.

(8) Valcarcel, A.; Ricart, J. M.; Clotet, A.; Illas, F.; Markovits, A.; Minot, C. Theoretical study of dehydrogenation and isomerisation reactions of propylene on Pt(111). *J. Catal.* **2006**, *241*, 115−122.

(9) Kubota, J.; Ichihara, S.; Kondo, J. N.; Domen, K.; Hirose, C. Reversibly adsorbed pi-bonded ethene on Pt(111) surfaces by infrared reflection absorption spectroscopy. *Langmuir* **1996**, *12*, 1926−1927.

(10) Lee, A. F.; Wilson, K. Fast x-ray spectroscopy study of ethene on clean and SO4 precovered Pt{111}. *J. Vac. Sci. Technol., A* **2003**, *21*, 563−568.

(11) Stair, P. C.; Somorjai, G. A. Adsorption of Acetylene on (111) Crystal-Face of Platinum - Detection of 2 Chemically Different Adsorption States by Low-Energy Electron-Diffraction. *Chem. Phys. Lett.* **1976**, *41*, 391−393.

(12) Aleksandrov, H. A.; Moskaleva, L. V.; Zhao, Z. J.; Basaran, D.; Chen, Z. X.; Mei, D. H.; Rosch, N. Ethylene conversion to ethylidyne on Pd(111) and Pt(111): A first-principles-based kinetic Monte Carlo study. *J. Catal.* **2012**, *285*, 187−195.

(13) Zaera, F.; Chrysostomou, D. Propylene on Pt(111) I. Characterization of surface species by infra-red spectroscopy. *Surf. Sci.* **2000**, *457*, 71−88.

(14) Koestner, R. J.; Frost, J. C.; Stair, P. C.; Vanhove, M. A.; Somorjai, G. A. Evidence for the Formation of Stable Alkylidyne Structures from C-3 and C-4 Unsaturated-Hydrocarbons Adsorbed on the Pt(111) Single-Crystal Surface. *Surf. Sci.* **1982**, *116*, 85−103.

(15) Zhou, Z. Y.; Kang, X. W.; Song, Y.; Chen, S. W. Ligand-Mediated Electrocatalytic Activity of Pt Nanoparticles for Oxygen Reduction Reactions. *J. Phys. Chem. C* **2012**, *116*, 10592−10598.

(16) Mirkhalaf, F.; Paprotny, J.; Schiffrin, D. J. Synthesis of metal nanoparticles stabilized by metal-carbon bonds. *J. Am. Chem. Soc.* **2006**, *128*, 7400−7401.

(17) Delamar, M.; Hitmi, R.; Pinson, J.; Saveant, J. M. Covalent modification of carbon surfaces by grafting of functionalized aryl radicals produced from electrochemical reduction of diazonium salts. *J. Am. Chem. Soc.* **1992**, *114*, 5883−5884.

(18) Ressler, T. WinXAS: a program for X-ray absorption spectroscopy data analysis under MS-Windows. *J. Synchrotron Radiat.* **1998**, *5*, 118−122.

(19) Ankudinov, A. L.; Ravel, B.; Rehr, J. J.; Conradson, S. D. Real-space multiple-scattering calculation and interpretation of x-ray-absorption near-edge structure. *Phys. Rev. B* **1998**, *58*, 7565−7576.

(20) Newville, M.; Boyanov, B. I.; Sayers, D. E. Estimation of uncertainties in XAFS data. *J. Synchrotron Radiat.* **1999**, *6*, 264−265.

(21) Creighton, J. A.; Eadon, D. G. Ultraviolet Visible Absorption-Spectra of the Colloidal Metallic Elements. *J. Chem. Soc., Faraday Trans.* **1991**, *87*, 3881−3891.

(22) Gerisch, M.; Heinemann, F. W.; Bogel, H.; Steinborn, D. Synthesis and characterization of platinum(II) complexes with terminal alkynes analogous to Zeise's salt - structure of [K(18-crown-6)][PtCl3(PhC CD)]center dot CH2Cl2. *J. Organomet. Chem.* **1997**, *548*, 247−253.

(23) Ding, S. W.; McDowell, C. A. Zeise's salt studied by high resolution solid state C-13 CPMAS and H-1 SPEDA NMR spectroscopy. *Chem. Phys. Lett.* **1997**, *268*, 194−200.

(24) Silverstein, R. M.; Bassler, G. C.; Morrill, T. C.: *Spectrometric Identification of Organic Compounds*, 5th ed.; Wiley: New York, 1991.

(25) Grogan, M. J.; Nakamoto, K. Infrared Spectra and Normal Coordinate Analysis of Metal-Olefin Complexes.I. Zeises Salt Potassium Trichloro (Ethylene) Platinate (2) Monohydrate. *J. Am. Chem. Soc.* **1966**, *88*, 5454−5460.

(26) Kang, X.; Chen, S. Electronic conductivity of alkyne-capped ruthenium nanoparticles. *Nanoscale* **2012**, *4*, 4183−4189.

(27) Kang, X.; Zuckerman, N. B.; Konopelski, J. P.; Chen, S. Alkyne-Functionalized Ruthenium Nanoparticles: Ruthenium-Vinylidene Bonds at the Metal-Ligand Interface. *J. Am. Chem. Soc.* **2012**, *134*, 1412−1415.

(28) Kaesz, H. D.; Saillant, R. B. Hydride Complexes of Transition-Metals. *Chem. Rev.* **1972**, *72*, 231−&.

(29) Peremans, A.; Tadjeddine, A. Vibrational Spectroscopy of Electrochemically Deposited Hydrogen on Platinum. *Phys. Rev. Lett.* **1994**, *73*, 3010−3013.

(30) Zayed, M. A.; Fischer, H. Investigation of novel organometallics by thermal spectroscopic methods. *J. Therm. Anal. Cal.* **2000**, *61*, 897−908.

(31) Spectral Database for Organic Compounds SDBS. http://sdbs.db.aist.go.jp/sdbs/cgi-bin/cre_index.cgi.

(32) Chen, W.; Zuckerman, N. B.; Konopelski, J. P.; Chen, S. W. Pyrene-Functionalized Ruthenium Nanoparticles as Effective Chemosensors for Nitroaromatic Derivatives. *Anal. Chem.* **2010**, *82*, 461−465.

(33) Chen, W.; Chen, S. W.; Ding, F. Z.; Wang, H. B.; Brown, L. E.; Konopelski, J. P. Nanoparticle-Mediated Intervalence Transfer. *J. Am. Chem. Soc.* **2008**, *130*, 12156−12162.

(34) Chen, W.; Zuckerman, N. B.; Lewis, J. W.; Konopelski, J. P.; Chen, S. W. Pyrene-Functionalized Ruthenium Nanoparticles: Novel Fluorescence Characteristics from Intraparticle Extended Conjugation. *J. Phys. Chem. C* **2009**, *113*, 16988−16995.

(35) Hostetler, M. J.; Wingate, J. E.; Zhong, C. J.; Harris, J. E.; Vachet, R. W.; Clark, M. R.; Londono, J. D.; Green, S. J.; Stokes, J. J.; Wignall, G. D.; Glish, G. L.; Porter, M. D.; Evans, N. D.; Murray, R. W. Alkanethiolate Gold Cluster Molecules with Core Diameters from 1.5 to 5.2 nm- Core and Monolayer Properties as a Function of Core Size. *Langmuir* **1998**, *14*, 17−30.

(36) Rowe, G. K.; Creager, S. E. Interfacial Solvation and Double-Layer Effects on Redox Reactions in Organized Assemblies. *J. Phys. Chem.* **1994**, *98*, 5500−5507.

(37) Aruna, I.; Mehta, B. R.; Malhotra, L. K.; Shivaprasad, S. M. Size dependence of core and valence binding energies in Pd nanoparticles: Interplay of quantum confinement and coordination reduction. *J. Appl. Phys.* **2008**, *104*, 064308.

(38) Duchesne, P. N.; Zhang, P. Local structure of fluorescent platinum nanoclusters. *Nanoscale* **2012**, *4*, 4199−4205.

(39) Duchesne, P. N.; Chen, G. X.; Zheng, N. F.; Zhang, P. Local Structure, Electronic Behavior, and Electrocatalytic Reactivity of CO-Reduced Platinum-Iron Oxide Nanoparticles. *J. Phys. Chem. C* **2013**, *117*, 26324−26333.

(40) Hostetler, M. J.; Wingate, J. E.; Zhong, C. J.; Harris, J. E.; Vachet, R. W.; Clark, M. R.; Londono, J. D.; Green, S. J.; Stokes, J. J.; Wignall, G. D.; Glish, G. L.; Porter, M. D.; Evans, N. D.; Murray, R. W. Alkanethiolate gold cluster molecules with core diameters from 1.5 to 5.2 nm: Core and monolayer properties as a function of core size. *Langmuir* **1998**, *14*, 17−30.

(41) Peters, T. B.; Bohling, J. C.; Arif, A. M.; Gladysz, J. A. C-8 and C-12 sp carbon chains that span two platinum atoms: The first structurally characterized 1,3,5,7,9,11-hexayne. *Organometallics* **1999**, *18*, 3261−3263.

(42) Watson, G. W.; Wells, R. P. K.; Willock, D. J.; Hutchings, G. J. Density functional theory calculations on the interaction of ethene with the {111} surface of platinum. *J. Phys. Chem. B* **2000**, *104*, 6439−6446.